IIETA International Information and Engineering Technology Association
Advancing the World of Information and Engineering

Mathematical Modelling of Engineering Problems
Vol. 13, No. 4, April, 2026, pp. 705-712
Journal homepage: http://iieta.org/journals/mmep

Effect of Friction Stir Welding Parameters on the Mechanical Performance and Microstructural Evolution of AA2024-O Aluminum Alloy Joints

Shaymaa Abdul Khader Al-Jumaili, Kussay Ahmed Subhi, Salam Abeed Dahe, Haider F. Mahmood*

Al-Mussaib Technical College, Al-Furat Al-Awsat Technical University, Babylon 51009, Iraq

Corresponding Author Email: haider.fawzi@atu.edu.iq

https://doi.org/10.18280/mmep.130408

Received: 20 January 2026
Revised: 18 April 2026
Accepted: 27 April 2026
Available online: 15 May 2026

Keywords:
friction stir welding, AA2024-O aluminum alloy, tool rotation speed, traverse speed, microstructural evolution, tensile strength, impact energy

ABSTRACT

Friction stir welding (FSW) is a solid-state joining process for aluminum alloys that is characterized by relatively low heat input and reduced defect formation. Among these alloys, AA2024-O presents considerable challenges during FSW because of its narrow process window and high susceptibility to defect formation. This study examines the effects of tool rotation speed, ranging from 500 to 1600 rpm, and traverse speed, ranging from 11 to 45 mm/min, on the mechanical properties and microstructure of AA2024-O FSW joints. The joints were evaluated through uniaxial tensile testing and impact testing. The stir-zone microstructure was analyzed using optical microscopy. The highest joint performance was obtained at 700 rpm and 18 mm/min, yielding a tensile strength of 188 MPa and an impact energy of 15.2 J, corresponding to 91–94% of the base-metal tensile strength and 82–84% of the base-metal impact energy, respectively. Moderate heat input promoted dynamic recrystallization and the formation of fine equiaxed grains measuring 5–12 μm, resulting in defect-free joints, whereas excessive or insufficient heat input led to grain coarsening, porosity formation, and reduced joint strength.

1. INTRODUCTION

The high strength-to-weight ratio of the latest aluminum alloys makes them ideal for aerospace, automotive, and weight-conscious structural designs [1]. Among these alloys, the AA2024-O aluminum alloy is recognized as the best-suited one in the presence of combined static and dynamic loading conditions. However, the mechanical properties of these high-performance materials are highly sensitive to microstructural features, which in turn depend on the process variables. Understanding the interrelationships among the process variables, microstructural development, and corresponding mechanical properties is necessary to ensure the reliability of joints in high-performance engineering applications.

Friction stir welding (FSW) is a modern joining technique invented by The Welding Institute (TWI) in 1991. It is a solid-state joining process in which a non-consumable rotating tool pin is plunged into the workpieces to be joined, where they meet and are traversed along the line of the study [2]. Because the tool pin rotates at a high speed, an axial force is generated, which creates localized frictional heat and softens the material around the tool pin. The softened material is urged to rotate from the face and backside of the pin, and a solid-state weld is formed.

This method is widely used to join heat-treatable aluminum alloys because a good joint can be attained with a low heat input. The final temperature of the FSW process was considerably lower than the working temperature of the parent material, resulting in less residual distortion, no cracks, and fine grains.

Aluminum (Al) and aluminum alloys are used in the fabrication of storage tanks, airplanes, automobiles, ships, heat exchangers, and in the building industry because of their good corrosion resistance, high strength-to-weight ratio, and easy fabrication [3, 4]. Many studies have investigated the effects of different process variables in FSW, such as rotation speed, traverse speed, plunge height, and dwell time, on the mechanical and microstructural properties of the welded joint. It is important to fully understand the relationship between the different process variables to obtain the maximum benefit from the joint properties.

FSW outcomes are known to be sensitive to variations in some parameters of the welding process, thus emphasizing the need for optimization, as discussed by several researchers [5, 6]. The parameters of the welding process, tool geometry, and design have a significant effect on the distribution of heat, flow patterns, microstructure, and quality of the bond of the material. Increasing the rotation speed results in the generation of more heat and, consequently, the displacement of a larger volume of material from the matrix. This will result in the weakening of the weld metal.

Zhou et al. [7] demonstrated that the tensile strength of Ti–6Al–4V alloy joints was significantly affected by the speed of rotation of the tool, with an optimal speed promoting better strength. This conclusion was supported by Sato and Kokawa [8], who suggested that a lower rotational speed leads to reduced heat input, which may cause inadequate bonding because of inadequate plasticization. A higher speed was also

suggested to promote a better surface appearance and dispersion of particles in composite materials.

Furthermore, the effects of the combination of rotational and traverse speeds on the heat input, grain refining mechanism, and development of defects were established. For instance, at higher traverse speeds, a low level of heat input may cause poor material flow and a reduction in the joint strength, whereas a high rotational speed may cause the development of porosity and intermetallic compounds.

Studies on aluminum alloys, such as AA5052, AA6082, and AA7020/AA6060 dissimilar joints, have shown that the mechanical properties are maximized when the parameters are carefully balanced. The traverse speed in some cases showed a stronger effect on the tensile strength and hardness than the rotational speed. Moreover, the plunge depth is a factor that influences material stirring and weld zone size and may lead to lack-of-fusion defects in case of overpenetration.

The thermal and mechanical environments that control FSW are mostly functions of the process parameters. Heat input, material flow, grain refinement, and weld integrity are highly sensitive to the tool shape and rotational and traverse speeds. As the rotational speed increases, the heat input increases; thus, plastic deformation and dynamic recrystallization are enhanced. However, a high heat input may result in grain growth and the development of porosity and intermetallic compounds. Higher traverse speeds result in lower heat input per unit length and lower welding times. This results in insufficient material plasticization. Current research suggests that the optimal weld performance is achieved when the rotational speed is moderate and the traverse speed is relatively low. In this case, a balanced thermal and mechanical environment results in the development of a refined microstructure and low defect density. Plunge depth is another factor that affects weld geometry and the possibility of defect generation.

Various studies have revealed the significance of the interaction between rotational speed and traverse speed in the heat input process and material flow in FSW. Cavaliere et al. [9] and Fonda and Bingert [10] showed that higher heat input at higher rotational speeds may increase defects and microstructural damage in the FSW process, and higher heat generation at lower traverse speeds may hinder material consolidation in the FSW process. Similar results in grain refinement and mechanical properties in aluminum alloys are observed by Aydın et al. [11], Kundu et al. [12], and Abu-Okail et al. [13].

However, recent research on aluminum alloys and similar materials has highlighted the significance of optimizing FSW parameters to produce sound joints without defects, along with improved mechanical properties [14-16]. However, most research on FSW has been conducted on heat-treated aluminum alloys. There is little research on how AA2024 performs in O-condition.

Although extensive research has been conducted on friction-stir welding of aluminum alloys, little research has investigated the relationship between the processing parameters of the rotational speed and traverse speed and the tensile and impact properties of AA2024-O. The current literature is dominated by results on heat-treated conditions.

This study continues a program to produce FSW parameters with specific features, to reinforce the response to achieve satisfactory conditions of mechanical performance and weld quality when the processing parameters are changed for (AA2024-O) aluminum alloy. The purpose is to identify the optimal parameters to improve the joint properties, which is important for the promotion of FSW in lightweight alloy structures in an industrial environment.

The novelty of this study lies in establishing an experimentally validated process–structure–property relationship for AA2024-O alloy under a wide range of rotational and traverse speeds, thereby providing an applied optimization framework suitable for industrial implementation.

2. MATERIALS AND METHODS

2.1 Materials and tool design

It had a cylindrical-conical k; the influence of FSW processing parameters on the mechanical and microstructural properties of welds in AA2024-O aluminum alloy (AA2024-O) was investigated. Wrought AA2024-O aluminum plates were used in this study. The chemical composition was determined using inductively coupled plasma optical emission spectroscopy (ICP-OES).

The chemical composition and mechanical properties of the AA2024-O alloy used in this study are consistent with those reported in the literature [17, 18], as shown in Table 1, and typical mechanical properties are listed in Table 2.

Table 1. Chemical composition of AA2024-O aluminum alloy (wt.%)

Element	Si	Fe	Cu	Mn	Mg	Cr	Zn	Ti
Standard	0.5 max	0.5 max	3.8–4.9	0.3–0.9	1.2–1.8	0.1	0.25	0.15
Measured	0.087	0.193	5.57	0.535	1.25	0.008	0.103	0.014

Table 2. Mechanical properties of AA2024-O aluminum alloy

	Ultimate Strength (MPa)	Yield Strength (MPa)	Modulus of Elasticity (GPa)
Standard	220	96	73.1
Measured	201	92	73.7

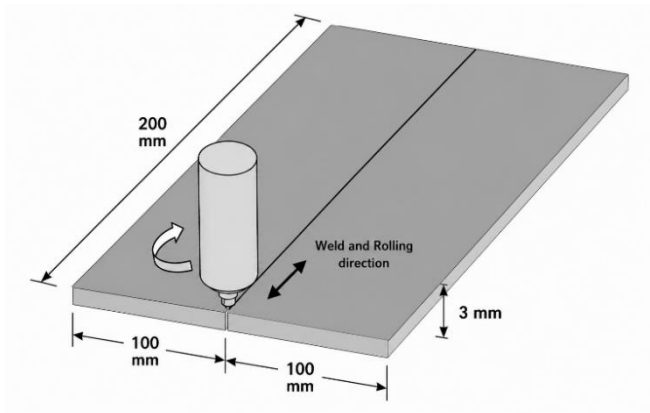

Figure 1. Schematic illustration of friction stir welding (FSW) by pin tool, showing a 200 mm × 200 mm workpiece with a thickness of 3 mm and the welding direction along the center line

Rectangular specimens with dimensions of 200 mm × 200 mm × 3 mm were fabricated using a wire-cutting machine. The

FSW was performed on an automated vertical milling machine with a dedicated clamping fixture. The FSW tool was made of tool steel K110 and then oil-quenched to enhance its hardness [19]. It had a cylindrical-conical pin profile with a pin diameter of 5.5 mm, a shoulder diameter of 25 mm, and a pin length of 6 mm. During the entire welding, the torch was tilted by 2°. A cylindrical–conical pin profile was selected to enhance material flow and reduce the likelihood of tunnel defects. The schematic representation of the FSW setup used in this study is shown in Figure 1.

2.2 Welding parameters

The process variables included rotational speeds of 500, 700, 1400, and 1600 rpm, whereas the traverse speeds included 11, 18, 35, and 45 mm/min. Table 3 summarizes these variables. These variables were chosen based on their expected effects on weld formation. The values of these variables were chosen based on pilot experiments conducted in addition to information regarding the thermal sensitivity of AA2024 alloys.

Table 3. Friction stir welding (FSW) process parameters and their selected levels

Parameters	Level 1	Level 2	Level 3	Level 4
Rotation speed [r/min]	500	700	1400	1600
Traverse speed [mm/min]	11	18	35	45

The selected parameter range was based on preliminary trials, in which lower rotational speeds (< 500 rpm) resulted in insufficient material flow, whereas higher speeds (> 1600 rpm) led to excessive flashing and porosity.

Figure 2. Optical microscope (Meiji Techno EMZ-5 / EMZ-8 Stereo Microscope) used for microstructural analysis

2.3 Metallographic analysis

For metallography, transverse cross-sections were taken perpendicular to the weld direction to include the stir zone (SZ), thermo-mechanically affected zone (TMAZ), heat-affected zone (HAZ), and the base material. The samples were then processed according to standard metallography techniques, which involved grinding using silicon carbide papers (240 to 2000 grit) successively. Further polishing was performed using a diamond suspension to produce a mirror finish. Microstructural examination was performed using an optical microscope (MEIJI). Etching was performed using Keller's reagent (2 mL HF, 3 mL HCl, 5 mL HNO_3, and 190 mL H_2O), following ASTM E407-76, to define the microstructural details of the weld areas. Microstructural examination was performed using an optical microscope (MEIJI), as illustrated in Figure 2.

2.4 Mechanical testing

Mechanical tests were performed in accordance with the ASTM standard to ensure the reliability and repeatability of the data. Tensile tests were performed using tensile specimens with standard dog-bone shapes and oriented along the welding direction, as illustrated in Figure 3. The tensile test was performed at room temperature using a 320 kN universal testing machine, where ultimate tensile strength and elongation were recorded.

For every welding condition, three tensile specimens and three impact specimens were tested. The values were recorded for the mean of the three measurements, with the standard deviation not exceeding ±3%.

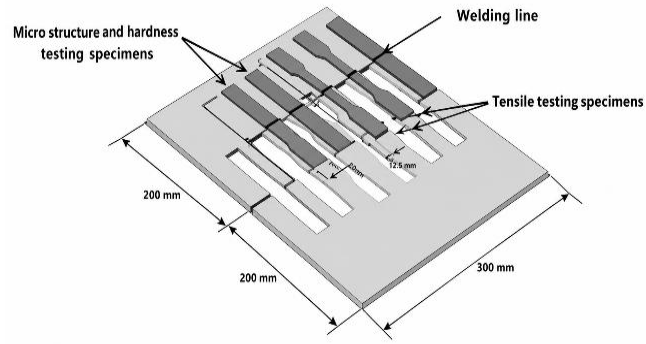

Figure 3. Schematic illustration of the friction stir welding (FSW) and the traverse testing specimens

3. RESULTS

3.1 Effect of friction stir welding parameters on tensile strength

The tensile strength characteristics of friction-stir-welded joints fabricated with different processing variables are listed in Table 4. The ultimate tensile strength is highly dependent on the combined processing variables of tool rotation speed and traverse speed, which can be related to the joint sensitivity to thermal and mechanical environments developed during the process. As shown in Table 4, an increase in the rotation speed from 500 rpm to 700 rpm with lower traverse speeds results in a noticeable improvement in the tensile strength; however, beyond that, a gradual reduction in joint performance is observed with an increase in rotation speed.

The highest tensile strength achieved was 188 MPa, or 93.5% of the base material strength, at a rotational speed of 700 rpm and traverse speed of 18 mm/min for FS6. This is because there was a balanced heat input that led to proper material plasticization, material flow, and dynamic recrystallization in the SZ to create a fine and defect-free microstructure. However, for samples produced at high rotational speeds of 1400–1600 rpm, especially at high

traverse speeds, the tensile strength was relatively low because of high heat input, which led to grain growth and porosity formation. At the same time, at low rotational speeds and high traverse speeds, there was less material flow and consolidation owing to low heat generation, resulting in a lower tensile strength for the joints. The lowest tensile strength was 132 MPa, or 65.7% of the base material strength, for the joint produced at 1600 rpm and a traverse speed of 45 mm/min for FS16.

Table 4. Effect of process parameters on tensile properties of friction stir welding (FSW) joints

Sample	Rotational Speed (rpm)	Traverse Speed (mm/min)	Ultimate Tensile Strength (MPa)	% of Base Material Strength	Elongation (%)
Base Material	-	-	201	100	12.5
FS1	500	11	160	79.6	7.8
FS2	500	18	172	85.6	8.3
FS3	500	35	155	77.1	6.9
FS4	500	45	145	72.1	6.2
FS5	700	11	175	87.1	8.9
FS6	700	18	188	93.5	9.4
FS7	700	35	168	83.6	7.5
FS8	700	45	154	76.6	6.8
FS9	1400	11	162	80.6	7.3
FS10	1400	18	170	84.6	8.0
FS11	1400	35	158	78.6	7.1
FS12	1400	45	143	71.1	6.0
FS13	1600	11	150	74.6	6.5
FS14	1600	18	157	78.1	7.2
FS15	1600	35	145	72.1	6.3
FS16	1600	45	132	65.7	5.5

3.2 Effect of friction stir welding parameters on impact resistance

The impact test results of the FSW joints with different welding parameters are listed in Table 5.

Table 5. Effect of process parameters on impact properties of friction stir welding (FSW) joints

Sample	Rotational Speed (rpm)	Traverse Speed (mm/min)	Impact Energy (J)	% of Base Material Impact Energy
Base Material	-	-	18.5	100
FS1	500	11	12.4	67.0
FS2	500	18	13.8	74.6
FS3	500	35	11.5	62.2
FS4	500	45	10.2	55.1
FS5	700	11	14.3	77.3
FS6	700	18	15.2	82.2
FS7	700	35	12.9	69.7
FS8	700	45	11.8	63.8
FS9	1400	11	12.0	64.9
FS10	1400	18	12.6	68.1
FS11	1400	35	11.2	60.5
FS12	1400	45	10.0	54.1
FS13	1600	11	11.2	60.5
FS14	1600	18	11.7	63.2
FS15	1600	35	10.3	55.7
FS16	1600	45	9.4	50.8

The obtained impact test results were consistent with the tensile strength results; specimen FS6 (700 rpm, 18 mm/min) represented the maximum impact energy of 15.2 J (82.2% of the base material impact resistance).

The impact behavior follows a trend similar to that of the tensile strength, indicating that joint toughness is strongly dependent on microstructural refinement and defect suppression in the SZ.

The reduction in impact energy for samples such as FS16 is attributed not only to grain coarsening but also to the presence of porosity, weak bonding, and possible oxide inclusions, which act as crack initiation sites under dynamic loading.

3.3 Microstructural analysis

Optical microscopy revealed various microstructures in the FSW samples under different process parameters.

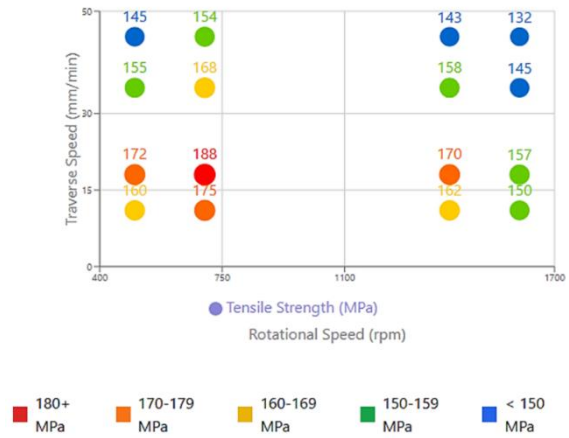

Figure 4. Optical micrographs of the stir zone (SZ) under selected friction stir welding (FSW) conditions

Table 6. Microstructural characteristics of friction stir welding (FSW) joints under different process parameters

Parameter Combination	Grain Structure in Stirred Zone	Average Grain Size (μm)	Defects Observed
500 rpm, 11 mm/min	Partially recrystallized, non-uniform grains	15–25	Tunnel defects at the advancing side
500 rpm, 18 mm/min	Better recrystallized, some non-uniformity	12–20	Minor lack of fill defects
700 rpm, 11 mm/min	Fine, equiaxed grains, good uniformity	8–15	Very few voids
700 rpm, 18 mm/min	Very fine, fully recrystallized, equiaxed grains	5–12	No significant defects
1400 rpm, 18 mm/min	Enlarged grains, evidence of excessive heat input	20–30	Some porosity
1600 rpm, 18 mm/min	Coarse grains, signs of overheating	25–40	Significant porosity and intermetallic compounds

Representative microstructures of the SZ under different welding conditions are presented in Figure 4. Figure 4 highlights the variation in grain size, recrystallization behavior, and defect formation under different heat input conditions.

The fine equiaxed grains observed at 700 rpm and 18 mm/min confirm the occurrence of dynamic recrystallization under balanced thermal conditions, which explains the superior mechanical performance.

Owing to the low rotational speed of 500 rpm and traverse speed of 11 mm/min, the heat input provided was insufficient to cause complete dynamic recrystallization. In addition, a nonuniform strain distribution resulted in partially recrystallized grain structures and tunnel defects.

The microstructural samples for various parameter combinations are presented in Table 6.

3.4 Hardness profiles

The hardness profile across the weld joint exhibited typical variations in different regions. The Vickers microhardness distribution across the weld zones for representative samples is shown in Figure 5.

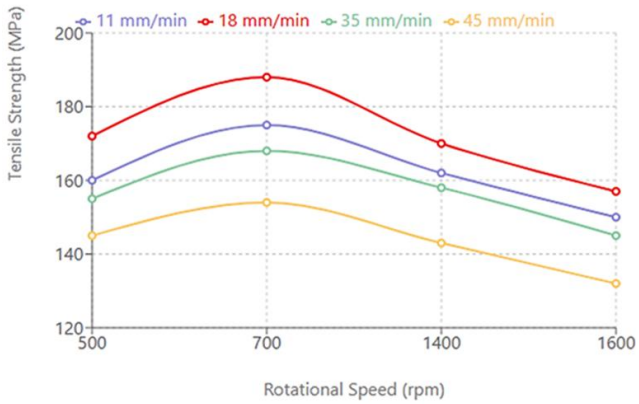

Figure 5. Vickers microhardness distribution across the weld zone under selected welding parameters

The hardness distribution also indicates a specific W-shape, with the minimum hardness values (HV) recorded within the SZ. More specifically, the hardness of the FS6 alloy was approximately 118 HV within the SZ, whereas the hardness of the FS16 alloy was approximately 90 HV, indicating thermal softening owing to excessive heat input. A quantitative comparison of the HV for the various weld regions is presented in Table 7.

Table 7. Representative hardness values (HV) across weld zones

Sample	SZ	TMAZ	HAZ	BM
FS6	118	105	95	120
FS16	90	85	80	120

Note: stir zone: SZ, thermo-mechanically affected zone: TMAZ, heat-affected zone: HAZ, BM: Base Metal.

To further clarify the relationship between the parameters and mechanical performance, a second-order regression model was proposed to link the tensile strength with the rotational and traverse speeds. The proposed model is expressed as follows:

$$TS = a + bN + cV + dN^2 + eV^2 + fNV \quad (1)$$

where, TS represents the tensile strength, N represents the rotational speed, V represents the traverse speed, and a, b, c, d, e, f are the regression coefficients.

The above model provides a predictive tool for the evaluation of the tensile strength for the considered parameter range.

4. DISCUSSION

4.1 Influence of rotational speed and traverse speed on mechanical properties

The analysis of the results shows that the mechanical properties of the AA2024-O friction-stir-welded joints are significantly dependent on the variations in the rotational and traverse speeds. This can be attributed to the effects of the rotational and traverse speeds on the thermal input and material flow. A suitable thermal input is required for the softening of the material and the stirring process.

At the lower speed of rotation (500 rpm), the frictional heat produced was inadequate for supporting substantial plastic flow and material mixing, thereby resulting in poor tensile and impact strength. This agrees with Sato and Kokawa [8], who mentioned that lower speed rotation results in less production of heat and hence improper bonding because of inadequate plastic flow. At too high a speed of rotation (1400–1600 rpm), excessive heat is produced, thereby deteriorating the quality of the bond. At this point, grain growth and the development of porosity and intermetallic compounds have been noted to have deteriorated the mechanical properties. Similar results have been documented by Dinaharan et al. [20], who attributed the deterioration in strength to excessive speed of rotation.

The traverse speed is another important factor that influences joint quality. At higher traverse speeds (35–45 mm/min), the rate of heat input per unit length is substantially reduced, which causes less material flow and consolidation in the SZ. Consequently, joints with poorer mechanical properties were formed, as supported by Cavaliere et al. [9], who reported that less heat input causes reduced joint quality, particularly when traverse speeds are high.

In contrast, the moderate rotational speed (700 rpm) and low traverse speed (18 mm/min) used together created the optimal conditions for both heat generation and cooling rate. This is important because it ensures that the material is properly plasticized. These optimal conditions were also noted in the latest research, which highlighted the need for a balanced thermal environment when performing FSW [21].

The mechanical behavior in welded joints is inextricably linked to the microstructural characteristics in the SZ. Microstructural observations using optical micrographs indicate that in optimal welded joints, there is an equiaxed and fully recrystallized microstructure with a fine grain size, whereas in sub-optimal welded joints, there is a coarse-grain microstructure or inhomogeneous grain distribution. The FS6 sample with a rotational speed of 700 rpm and a traverse speed of 18 mm/min exhibited the smallest grain size with minimum defects, indicating higher tensile and impact strengths with values of 188 MPa and improved impact resistance, respectively. The predicted tensile strength from the proposed model (Eq. (1)) for the optimal parameters (700 rpm, 18 mm/min) is consistent with the experimental value (188 MPa),

confirming the model's validity. The sensitivity of the impact resistance to the processing variables indicates the significance of energy absorption mechanisms in structural materials. Issues associated with the impact response and damage development have been addressed by recent studies on the dynamic impact response of composite materials, as the architecture of materials, as well as the processing variables, have a significant influence on the resistance to impact [22].

4.2 Microstructural evolution and its relation to mechanical properties

The O-temper properties of AA2024, including decreased strength and increased ductility, are compared with other heat treatment tempers, such as T6. This facilitates the flow of materials during FSW but increases the rate of thermal softening in AA2024. Hence, the balance of heat input and plastic deformation is more important for AA2024-O than for other precipitation-hardened alloys.

The main driving force behind grain refinement during FSW is the dynamic recrystallization process. This occurs when the thermal and deformation conditions are favorable.

Favorable values of rotational speed can bring about this process, resulting in a refined grain structure and improved joint strength, as observed by Zhou et al. [7]. The results of the current study are in agreement with those.

The fine microstructure developed in the SZ under optimal welding conditions can be attributed to a balanced thermal input, which promotes dynamic recrystallization and resists grain growth. This result corroborates the findings of earlier microstructural studies on the friction-stir welding of aluminum alloys, in which dynamic recrystallization was shown to be the primary factor influencing grain development [7, 14, 23]. The fine and equiaxed-grain microstructure developed in the SZ improves the load-carrying capability and toughness, thus explaining the superior mechanical properties in the current study.

At high rotational speeds (1400 and 1600 rpm), a significant amount of heat led to grain coarsening during the cooling process, thereby negatively affecting the mechanical properties. This agrees with the observations of Moshwan et al. [23], who stated that high thermal exposure in FSW can offset the advantages gained through grain refinement. The effect of the welding process variables on microstructural development, as observed in this experiment, agrees with the observations of Al-Jumaili et al. [2].

4.3 Defect formation mechanisms

The formation of defects in friction-stir-welded joints can be significantly influenced by improper setting of the rotational and traverse speeds. Low rotational speed and high traverse speed result in low heat input, thereby preventing the material from being sufficiently plasticized, resulting in the formation of tunnel defects and voids, mainly on the advancing side of the weld joint [24, 25].

In contrast, excessively high rotational speeds result in excessive heat input, which promotes the creation of porosity and intermetallic compounds that act as stress concentrations, thus weakening the joint. Various researchers have observed defect mechanisms related to high heat input [9, 26, 27]. In addition, incorrect plunge height together with undesirable rotational and traverse speeds may result in the worsening of defect creation, as observed by Iqbal et al. [25].

4.4 Optimization of friction stir welding parameters for AA2024-O Aluminum alloy

Based on a complete analysis of the mechanical properties, microstructure, and defects, the optimum FSW process parameters for AA2024-O aluminum alloy were found to be a rotation speed of 700 rpm and a traverse speed of 18 mm/min. At these optimum process parameters, the maximum efficiency of the weld tensile joint was 93.5%, compared to the parent material, along with an impact strength of 82.2%, compared to the parent material. Impact performance is expressed as relative impact on energy rather than efficiency to avoid ambiguity.

From an engineering perspective, this set of process parameters provides a well-optimized trade-off between the quality of the joints and the process, making it ideal for the industrial production of lightweight aluminum structure components. The results of the present study confirm earlier studies on aluminum alloy optimization [28, 29] as well as recent studies on the significance of the heat input–material flow rate process parameter interaction to attain the maximum joint efficiency [20, 30]. Similar trends have also been reported by Raut et al. [31] for aluminum alloys and by Chakravarthi et al. [32] for titanium alloys.

5. CONCLUSIONS

The results of this study show that the mechanical response of friction-stir-welded AA2024-O alloy is significantly dependent on the combined effects of heat input and material flow conditions. A balanced condition of process parameters is necessary for achieving defect-free welds with refined microstructures.

The results indicate that moderate rotational speeds and relatively low traverse speeds are favorable for stable plastic deformation and uniform dynamic recrystallization in the SZ, thereby improving the mechanical and impact properties. Excessive heat input and high rotational speeds result in microstructural coarsening and defects. In contrast, low heat input and high traverse speeds result in poor consolidation.

The results of this investigation have significant implications for the control of parameters to produce reliable welds in AA2024-O. The findings can be used as a reference for selecting the parameters for friction-stir welding and may also support the development of future models for parameter optimization and process control in friction stir welding.

REFERENCES

[1] Fnides, M., Bensana, T., Fnides, B., Mihoub, M. (2023). Experimental analysis of the mechanical characteristics of aluminum alloys ($AlSi_8Cu_3$). Annales de Chimie - Science des Matériaux, 47(4): 209-218. https://doi.org/10.18280/acsm.470403

[2] Al-Jumaili, S.A.K., Al-Jburi, A.H., Dahe, S.A., Al-Mamoori, R.A. (2020). Investigate of the influence for multiple resistance welding currents in austerities nickel-chromium alloys on welded joints mechanical characteristics. Periodicals of Engineering and Natural Sciences (PEN), 8: 423-429. https://doi.org/10.21533/pen.v8.i1.1059

[3] Thangarasu, A., Murugan, N., Dinaharan, I., Vijay, S.J.

(2014). Effect of tool rotational speed on microstructure and microhardness of AA6082/TiC surface composites using friction stir processing. Applied Mechanics and Materials, 592: 234-239. https://doi.org/10.4028/www.scientific.net/AMM.592-594.234

[4] Karthikeyan, L., Senthil Kumar, V.S. (2011). Relationship between process parameters and mechanical properties of friction-stir-processed AA6063-T6 aluminum alloy. Materials & Design, 32: 3085-3091. https://doi.org/10.1016/j.matdes.2010.12.049

[5] Jayaraman, M., Sivasubramanian, R., Balasubramanian, V., Babu, S. (2009). Optimisation of friction stir welding process parameters to weld cast aluminium alloy A413 – An experimental approach. International Journal of Cast Metals Research, 22(5): 367-373. https://doi.org/10.1179/174313309X380404

[6] Lin, P.C., Pan, J., Pan, T. (2008). Failure modes and fatigue life estimations of spot friction welds in lap-shear specimens of aluminum 6111-T4 sheets. Part 2: Welds made by a flat tool. International Journal of Fatigue, 30(1): 90-105. https://doi.org/10.1016/j.ijfatigue.2007.02.017

[7] Zhou, L., Liu, H.J., Liu, Q.W. (2010). Effect of rotation speed on microstructure and mechanical properties of Ti–6Al–4V friction stir welded joints. Materials & Design, 31(5): 2631-2636. https://doi.org/10.1016/j.matdes.2009.12.014

[8] Sato, Y.S., Kokawa, H. (2001). Distribution of tensile property and microstructure in friction stir weld of 6063 aluminum. Metallurgical and Materials Transactions A, 32(12): 3023-3031. https://doi.org/10.1007/s11661-001-0177-8

[9] Cavaliere, P., Squillace, A., Panella, F. (2008). Effect of welding parameters on mechanical and microstructural properties of AA6082 joints produced by friction stir welding. Journal of Materials Processing Technology, 200(1-3): 364-372. https://doi.org/10.1016/j.jmatprotec.2007.09.050

[10] Fonda, R.W., Bingert, J.F. (2006). Precipitation and grain refinement in a 2195 Al friction stir weld. Metallurgical and Materials Transactions A, 37(12): 3593-3604. https://doi.org/10.1007/s11661-006-1054-2

[11] Aydın, H., Bayram, A., Durgun, I. (2010). The effect of post-weld heat treatment on the mechanical properties of 2024-T4 friction stir-welded joints. Materials & Design, 31(5): 2568-2577. https://doi.org/10.1016/j.matdes.2009.11.030

[12] Kundu, J., Ghangas, G., Rattan, N., Sharma, S.K. (2017). Effect of different parameters on heat generation and tensile strength of FSW AA5083 joint. International Journal of Current Engineering and Technology, 7(3): 1170-1174.

[13] Abu-Okail, M., Abu-Oqail, A., Ata, M.H. (2020). Effect of friction stir welding process parameters with interlayer strip on microstructural characterization and mechanical properties. Journal of Failure Analysis and Prevention, 20(1): 173-183. https://doi.org/10.1007/s11668-020-00813-0

[14] Li, Y., Sun, D., Gong, W. (2019). Effect of tool rotational speed on the microstructure and mechanical properties of bobbin tool friction stir welded 6082-T6 aluminum alloy. Metals, 9(8): 894. https://doi.org/10.3390/met9080894

[15] Khalafe, W.H., Sheng, E.L., Bin Isa, M.R., Omran, A.B., Shamsudin, S.B. (2022). The effect of friction stir welding parameters on the weldability of aluminum alloys with similar and dissimilar metals. Metals, 12(12): 2099. https://doi.org/10.3390/met12122099

[16] Kumar, R., Salah, A.N., Kant, N., Singh, P., Hashmi, A.W., Malla, C. (2022). Effect of FSW process parameters on mechanical properties and microstructure of dissimilar welded joints of AA2024 and AA6082. Materials Today: Proceedings, 50: 1435-1441. https://doi.org/10.1016/j.matpr.2021.09.007

[17] Ahmed, S., Rahman, R.A.U., Awan, A., Ahmad, S., et al. (2022). Optimization of process parameters in friction stir welding of aluminum 5451 in marine applications. Journal of Marine Science and Engineering, 10(10): 1539. https://doi.org/10.3390/jmse10101539

[18] Chandla, N.K., Kant, S., Goud, M.M. (2023). A review on mechanical properties of stir cast Al-2024 metal matrix composites. Advances in Materials and Processing Technologies, 9(3): 948-969. https://doi.org/10.1080/2374068X.2022.2106670

[19] Al-Jumaili, S.A.K., Hawas, M.N., Al-Gburi, H. (2023). Evaluation of the impact of surface treatment on the turbine blade performance. Jordan Journal of Mechanical and Industrial Engineering, 17(3): 421-427. https://doi.org/10.59038/jmie/170311

[20] Dinaharan, I., Kalaiselvan, K., Vijay, S.J., Raja, P. (2012). Effect of material location and tool rotational speed on microstructure and tensile strength of dissimilar friction stir welded aluminum alloys. Archives of Civil and Mechanical Engineering, 12(4): 446-454. https://doi.org/10.1016/j.acme.2012.08.002

[21] Ismail, A., Zulkipli, F.N., Awang, M., Ab Rahman, F., Khalid, P.Z.M., Baharudin, B.A. (2021). Optimum welding parameters for friction stir welded AA6063 pipe butt joint using the Taguchi method. Transactions on Maritime Science, 10(2): 404-413. https://doi.org/10.7225/toms.v10.n02.011

[22] Faisal, B.M., Abed, K.A., Mohammed, A.A., Hussein, E.K., Sharaf, H.K., Santos, T., Santos, C. (2024). Investigation of the high velocity impact test on the curved glass fiber reinforced plastic (GFRP) composites using explicit dynamics analysis. International Journal on Advanced Science, Engineering & Information Technology, 14(6): 2084-2089. https://doi.org/10.18517/ijaseit.14.6.10417

[23] Moshwan, R., Yusof, F., Hassan, M.A., Rahmat, S.M. (2015). Effect of tool rotational speed on force generation, microstructure and mechanical properties of friction stir welded Al–Mg–Cr–Mn (AA 5052-O) alloy. Materials & Design, 66: 118-128. https://doi.org/10.1016/j.matdes.2014.10.043

[24] Hema, P., Ravindranath, K. (2017). Prediction of effect of process parameters on friction stir welded joints of dissimilar Aluminium alloy AA2014 & AA6061 using taper pin profile. Materials Today: Proceedings, 4(2): 2174-2183. https://doi.org/10.1016/j.matpr.2017.02.064

[25] Iqbal, M.P., Vishwakarma, R.K., Pal, S.K., Mandal, P. (2023). Influence of plunge depth during friction stir welding of aluminum pipes. Proceedings of the Institution of Mechanical Engineers, Part B: Journal of Engineering Manufacture, 237(13): 2085-2096. https://doi.org/10.1177/0954405420949754

[26] Giraud, L., Robe, H., Claudin, C., Desrayaud, C.,

Bocher, P., Feulvarch, E. (2016). Investigation into the dissimilar friction stir welding of AA7020-T651 and AA6060-T6. Journal of Materials Processing Technology, 235: 220-230. https://doi.org/10.1016/j.jmatprotec.2016.04.025

[27] Salih, O.S., Ou, H., Sun, W. (2023). Heat generation, plastic deformation and residual stresses in friction stir welding of aluminium alloy. International Journal of Mechanical Sciences, 238: 107827. https://doi.org/10.1016/j.ijmecsci.2022.107827

[28] Dursun, T., Soutis, C. (2014). Recent developments in advanced aircraft aluminium alloys. Materials & Design, 56: 862-871. https://doi.org/10.1016/j.matdes.2013.12.002

[29] Mosleh, A.O., Yakovtseva, O.A., Kishchik, A.A., Kotov, A.D., Moustafa, E.B., Mikhaylovskaya, A.V. (2023). Effect of coarse eutectic-originated particles on the microstructure and properties of the friction stir-processed Al-Mg-Zr-Sc-based alloys. JOM, 75(8): 2989-3000. https://doi.org/10.1007/s11837-023-05712-x

[30] Djouider, F., Alhawsawi, A., Elmoujarkach, E., Banoqitah, E., Alharazi, M., Moustafa, E.B. (2023). The role of friction stir processing parameters and hybrid ZrC/WC reinforcement particles in improving the surface composite dissimilar matrix's dynamic behavior and microstructure refinement. Coatings, 13(8): 1393. https://doi.org/10.3390/coatings13081393

[31] Raut, N., Yakkundi, V., Sunnapwar, V., Medhi, T., Jain, V.K.S. (2022). A specific analytical study of friction stir welded Ti-6Al-4V grade 5 alloy: Stir zone microstructure and mechanical properties. Journal of Manufacturing Processes, 76: 611-623. https://doi.org/10.1016/j.jmapro.2022.02.036

[32] Chakravarthi, G., Giridharan, K., Stalin, B., Padmanabhan, S., Sekar, S., Nagaprasad, N., Jule, L.T., Krishnaraj, R. (2022). Investigation on the effect of process parameters on mechanical and microstructural properties of AA8011 similar FSW weld joints. Advances in Mechanical Engineering, 14(7): 16878132221112146. https://doi.org/10.1177/16878132221112146

NOMENCLATURE

d	Pin diameter, mm
D	Tool shoulder diameter, mm
E	Modulus of elasticity, GPa
F	Axial force, N
H	Plate thickness, mm
HV	Vickers hardness, kgf·mm^{-2}
L	Weld length, mm
N	Tool rotational speed, rpm
Q	Heat input, J

Greek symbols

α	Thermal diffusivity, m^2·s^{-1}
β	Thermal expansion coefficient, K^{-1}
θ	Tool tilt angle, degree (°)
μ	Dynamic viscosity, kg·m^{-1}·s^{-1}
ρ	Density, kg·m^{-3}
σ	Tensile stress, MPa

Subscripts

BM	Base material
FSW	Friction stir welded joint
HAZ	Heat affected zone
SZ	Stir zone
TMAZ	Thermo-mechanically affected zone